Growth Factors, October 2012; 30(5): 333–343

informa
healthcare

Osteogenic response of human adipose-derived stem cells to BMP-6, VEGF, and combined VEGF plus BMP-6 *in vitro*

YI ZHANG[1,2,*], VEDAVATHI MADHU[1,*], ABHIJIT S. DIGHE[1], JAMES N. IRVINE Jr.[1], & QUANJUN CUI[1]

[1]*Department of Orthopaedic Surgery, University of Virginia, Charlottesville, VA, USA, and* [2]*Department of Orthopaedic Surgery, The First Affiliated Hospital of Zhengzhou University, Zhengzhou, Henan, People's Republic of China*

(*Received 19 June 2012; revised 7 August 2012; accepted 9 August 2012*)

Abstract

Exogenous addition of three factors—mesenchymal stem cells (MSCs), vascular endothelial growth factor (VEGF), and bone morphogenetic proteins (BMPs)—has proven to be more beneficial than delivery of any single factor for fracture repair in animal models. We studied the osteogenic differentiation of human adipose-derived stem cells (hADSCs) in the presence of VEGF, BMP-6, or VEGF plus BMP-6 to better understand their enhancement of osteoblastic differentiation of MSCs. The VEGF plus BMP-6 group demonstrated an additive effect on the enhancement of mineralization and expression of *ALP* and *Msx2* genes. Unlike VEGF or BMP-6 alone, the combination of VEGF and BMP-6 significantly enhanced the expression of *COL1A1*, osterix, and *Dlx5* genes. The data indicate that a cross-talk between VEGF and BMP-6 signaling pathways enhances osteogenic differentiation of hADSCs.

Keywords: *Mesenchymal stem cells, VEGF, BMP-6, osteogenesis, bone repair*

Introduction

Treatment of large bone defects and nonunion fractures continues to be a challenging clinical problem. Novel research in tissue engineering may provide new treatment options geared at combining bioresorbable scaffolds, stem cells, and growth factors to generate new bone growth at targeted sites. Many growth factors have been studied, but bone morphogenetic proteins (BMPs) have proven to play a critical role in the regeneration process of bone formation. They induce an intracellular signal following their binding to a cell surface receptor which upregulates a cascade of events inside the cell. These intracellular processes cause differentiation of progenitor cells into chondrocytes and osteoblasts, which aid in new bone formation by enhancing endochondral ossification (Hanada et al. 2001). Bone is a highly dynamic tissue requiring a constant supply of blood and nutrients to keep it healthy and strong. Their remarkably vascularized structure has led to bone repair strategies that are focused on increasing angiogenesis at the defect site. In recent years, vascular endothelial growth factor (VEGF) has been a popular small molecule in many areas of research seeking increased amounts of blood supply to help in new tissue formation. VEGF has been well investigated by orthopedists and is known for its role in osteogenesis and bone repair (Geiger et al. 2005).

The combination of VEGF, an angiogenic growth factor, plus osteogenic factors such as BMP-2 (Peng et al. 2005; Patel et al. 2008; Samee et al. 2008; Hou et al. 2009; Kempen et al. 2009; Young et al. 2009) and BMP-4 (Peng et al. 2002; Huang et al. 2005; Kubo et al. 2009; Li et al. 2009; Matsumoto et al. 2009) reportedly has a synergistic impact on their

Correspondence: Quanjun Cui, Department of Orthopaedic Surgery, University of Virginia, P.O. Box 800159, Charlottesville, VA 22908, USA. Tel: 1 434 243 0236. Fax: 1 434 243 0242. E-mail: qc4q@hscmail.mcc.virginia.edu
*The authors contributed equally to this work.

ISSN 0897-7194 print/ISSN 1029-2292 online
DOI: 10.3109/08977194.2012.720574

induction of bone repair. Studies have proven that BMP-6 and BMP-9 have the greatest potential for bone regeneration (Li et al. 2003b; Kang et al. 2004). However, BMP-9 is also reported to inhibit angiogenesis by binding to the Alk1 receptor (Scharpfenecker et al. 2007). Our laboratory has shown that co-expression of the human VEGF gene with human BMP-6 gene (Cui et al. 2010) or with human LIM mineralization protein-1 (LMP-1) gene enhances osteogenesis induced by mouse bone marrow-derived stem cells (BMSCs) *in vivo* (Wang et al. 2011). LMP-1 is a known downstream modulator of the BMP-6 signaling pathway (Boden et al. 1998). It is reported that VEGF's synergistic role in BMP-induced osteogenesis is cell-type dependent (Li et al. 2009). We sought to determine whether the combination of VEGF and BMP-6 enhances osteoblastic differentiation of mesenchymal stem cells (MSCs) using human adipose-derived stem cells (hADSCs) *in vitro*.

Methods

Cell culture

hADSCs were purchased from a commercial source (Lonza, Basel, Switzerland) and grown in Dulbecco's Modified Eagle's Medium (Gibco BRL, Gaithersburg, MD, USA) containing 10% fetal bovine serum (Hyclone Laboratories, Logan, Utah, USA), 50 μg/ml sodium ascorbate, 100 IU/ml penicillin G, and 100 μg/ml streptomycin of culture media in a humidified atmosphere of 5% carbon dioxide at 37°C. The medium was designated as basal medium (BM) and to induce osteogenic differentiation of hADSCs, 10 mM β-glycerophosphate and 10^{-7} M dexamethasone were added to BM to prepare osteogenic medium (OM). The human recombinant proteins of BMP-2, BMP-4, BMP-6; VEGF (ProSpec, Ness-Ziona, Israel); and BMP-9 (Assay Designs/Enzo Life Sciences, Farmingdale, NY, USA) were immediately (day 0) added to OM at specified concentrations. All experiments were conducted with passage 8 (p-8) hADSCs at the starting cell density of 5000 cells/cm^2.

Morphology and multilineage potential of hADSCs

The hADSCs were plated in a 24-well plate and grown for 4 days. At day 5, cells were stained with fluorescein isothiocyanate (FITC)-labeled phalloidin (Sigma, St. Louis, MO, USA) to stain F-actin filaments in order to visualize the cytoplasm as well as with 4′,6-diamidino-2-phenylindole (DAPI; Sigma) to stain the nuclei of the hADSCs. Briefly, cells were washed with phosphate-buffered saline (PBS) and fixed in 3.5% formaldehyde for 15 min. Cells were then washed three times with PBS and permeabilized with 0.1% Triton X-100 for 2 min and washed three times with PBS. After washing the cells, they were stained with 1 μg/ml FITC-conjugated phalloidin for 40 min at room temperature and at the same time 1 μg/ml DAPI was also added to stain the nuclei. Following incubation, cells were washed extensively with PBS to remove unbound dye and then visualized under a microscope.

To determine whether the p-8 hADSCs were capable of differentiation along an adipogenic lineage, the cells were cultured in BM containing 10^{-4} M dexamethasone for 14 days to induce adipogenesis. The differentiated cells were stained with Sudan IV, a stain for fat, counterstained with hematoxylin, and visualized by light microscopy (Li et al. 2003a). To test the ability of the p-8 hADSCs to differentiate along the osteogenic lineage, the cells were grown in OM for 14 days. The differentiated cells were stained with Alizarin Red solution and visualized under a microscope (Krause et al. 2011).

Expression of MSCs markers as well as VEGF, TGF, and BMP receptors

The hADSCs were grown in BM for 10 days and then trypsinized. Next, they were washed three times with PBS + 1% BSA (bovine serum albumin) to prepare a homogenous cell suspension. About 1×10^6 hADSCs were incubated in the dark for 30 min with the specific monoclonal antibody for staining the surface receptor. The following monoclonal antibodies (eBiosciences, San Diego, California, USA) were used according to manufacturer's instructions: PE-labeled anti-CD105 clone SN6, PerCPCy5.5-labeled anti-CD90 clone eBio5E10, PerCP-labeled anti-CD73 clone AD2, FITC-labeled anti-CD146 clone P1H12, FITC-labeled anti-CD45 clone 2D1, FITC-labeled anti-CD34 clone 4H11, and APC-labeled anti-ALP clone B4-78 (R&D Systems, Minneapolis, MN, USA). The cells were washed three times with PBS + 1% BSA and analyzed using an FACScalibur flow cytometer (BD Biosciences, San Jose, California, MD, USA) and data were analyzed using FlowJo software (Tree Star, Ashland, OR, USA). In order to achieve uniformity in the data obtained using different MSCs, the International Society for Cellular Therapy (ISCT) has proposed guidelines (Dominici et al. 2006) based on cell surface expression of receptors. The typical phenotype of the MSCs is as follows: CD 105 + CD90 + CD73 + CD45 − CD34 − CD14 − /CD11b − CD79α − /CD19 − . As our knowledge of surface markers evolves, some of the details contained in these guidelines may have to be adjusted to reflect the characteristics of the cells (Tallone et al. 2011). We tested CD146 expression as CD146-expressing MSCs could generate complete miniaturized bone organ *in vivo* (Sacchetti et al. 2007).

mRNA expression of VEGF receptors (VEGFR1 and VEGFR2), tumor growth factor (TGF) receptors (Alk1 and Alk5), and BMP receptors (Alk2, Alk3, and

Table I. List of primer sequences for conventional PCR

Gene	Forward or reverse primer	Primer sequence
Alk1	Forward	5′-AGCAGGCCTGTCTCAGGA-3′
Alk1	Reverse	5′-CCTGGGAGGTAGACGTTGC-3′
Alk2	Forward	5′-CCCAGCTGCCCACTAAAG-3′
Alk2	Reverse	5′-CGCCTTTTAAATTTTCGGAGA-3′
Alk3	Forward	5′-GGACGAAAGCCTGAACAAAA-3′
Alk3	Reverse	5′-GCAATTGGTATTCTTCCACGA-3′
Alk5	Forward	5′-AACGTCAGGTTCTGGCTCA-3′
Alk5	Reverse	5′-GAATATCTTAACAGCAACTTCTTCTCC-3′
Alk6	Forward	5′-ATCAGGCCTCCCTCTGCT-3′
Alk6	Reverse	5′-CACTTTCACAGCTACCTTTTCG-3′
VEGFR2	Forward	5′-GGAAGCTCCTGAAGATCTGT-3′
VEGFR2	Reverse	5′-GAGGATATTTCGTGCCGC-3′
VEGFR1	Forward	5′-CTGGGAGGAAGAAGAGGGTAGGTG-3′
VEGFR1	Reverse	5′-CGAGGGCGGGGGCGATTTAT-3′
GADPH	Forward	5′-CATGTTCCAATATGATTCCACC-3′
GADPH	Reverse	5′-GATGGGATTTCCATTGATGAC-3′

Alk6) was determined using the cDNA template and gene-specific primers by conventional polymerase chain reaction (PCR). The amplified DNA products from the PCRs were resolved in a 1% agarose gel and stained with ethidium bromide. The primer sequences used can be seen in Table I.

Alizarin Red staining

The staining was performed as described elsewhere (Gregory et al. 2004) to quantify the mineralization. hADSCs were grown in a 24-well plate in BM or OM or OM supplemented with different growth factors for 4 weeks. The medium from each well was replaced twice a week. After 2, 3, and 4 weeks, the medium was removed from the wells, the wells were washed with 450 μl of PBS, and fixed in 400 μl of 10% (v/v) formaldehyde for 15 min. After removing the formaldehyde, the wells were washed twice with 1 ml of sterilized water; 400 μl of 40 mM Alizarin Red stain solution of pH 4.1 was placed in each well for 20 min. After removing the Alizarin Red stain solution, the wells were washed 4 times with sterilized water; 200 μl of 10% (v/v) acetic acid was placed in the wells for 30 min. The solid and liquid mass inside each of the wells was placed into individual centrifuge tubes, heated at 85°C for 10 min, and then transferred to ice for 5 min. The mixture in each tube was centrifuged at 15,000 rpm for 15 min, and 250 μl of supernatant was removed to a new 1.5-ml centrifuge tube. To neutralize the acid, 100 μl of 10% (v/v) NH_4OH was added to the wells, and 150 μl aliquots of the supernatant were read in triplicate at 405 nm in a 96-well format using opaque-walled, transparent-bottom plates. The experiment was done in triplicates. The dissolution of Alizarin Red in all the samples was complete at all time points, days 14, 21, and 28, respectively.

mRNA expression of osteoblastic marker genes

Total RNA was extracted and then purified using the RNeasy® kit (QIAGEN Sciences, Qiagen, Valencia,

Table II. List of primer sequences for Real Time PCR.

Gene	Forward or reverse primer	Primer sequence
ALP	Forward	5′-ACCATTCCCACGTCTTCACATTTG-3′
ALP	Reverse	5′-AGACATTCTCTCGTTCACCGCC-3′
Col I	Forward	5′-GGACACAATGGATTGCAAGG-3′
Col I	Reverse	5′-TAACCACTGCTCCACTCTGG-3′
OCN	Forward	5′-CAGGCGCTACCTGTATCAAT-3′
OCN	Reverse	5′-CTGGAGTTTATTTGGGAGCA-3′
BSP	Forward	5′-AGCCAGGACTCCATTGACTCGAAC-3′
BSP	Reverse	5′-GTTTCAGCACTCTGGTCATCCAGC-3′
Runx2	Forward	5′-AGATGATGACACTGCCACCTCTG-3′
Runx2	Reverse	5′-GGGATGAAATGCTTGGGAACTGC-3′
Osterix	Forward	5′-GGCAAGAGGTTCACTCGTTC-3′
Osterix	Reverse	5′-GTCTGACTGGCCTCCTCTTC-3′
Msx2	Forward	5′-GCCATTTTCAGCTTTTCCAG-3′
Msx2	Reverse	5′-CCCTGAGGAAACACAAGACC-3′
Dlx5	Forward	5′-CAACTTTGCCCGAGTCTTCA-3′
Dlx5	Reverse	5′-GTTGAGAGCTTTGCCATAGGAA-3′

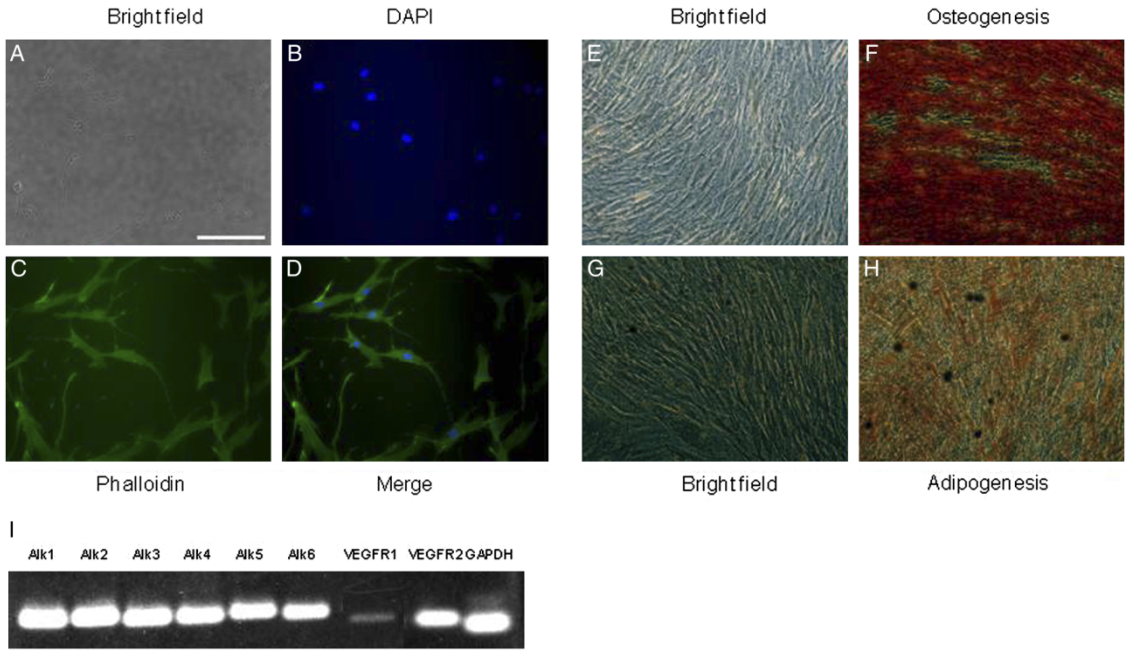

Figure 1. Characteristics of hADSCs. The hADSCs were stained with DAPI (B) and FITC-conjugated phalloidin (C) to visualize cell morphology (A–D) under a microscope. The images obtained were overlapped to create an image (D) showing green actin filaments and blue nuclei in the hADSCs. The ability of hADSCs to differentiate into osteogenic and adipogenic lineages (E–H) was assayed by staining with Alizarin Red (F) and Sudan IV (H), respectively. Expression of VEGF, TGF, and BMP receptors was determined by PCR using gene-specific primers followed by agarose gel electrophoresis and staining with ethidium bromide solution (I). The bar represents 200 μm.

CA). The RNase-free DNase was used to remove unwanted DNA. The iScript™ Select cDNA Synthesis Kit (Bio-Rad Laboratories, Hercules, CA, USA) was used to synthesize the cDNA according to the instructions provided by the manufacturer. The mRNA expression of various osteogenic markers was quantitatively determined using the iQ™ SYBR® Green Supermix Kit (Bio-Rad Laboratories) and the iQ™ 5 Multicolor Real-Time PCR Detection System (Bio-Rad Laboratories). The PCRs were performed using the cDNA (112.5 ng total RNA equivalents) and 25 μl of the iQ™ SYBR® Green Supermix supplemented with the forward and reverse primers (300 nm/l each). The PCR protocols required activation of AmpliTaq Gold DNA polymerase followed by 40 cycles of denaturation at 94°C for 30 s, annealing at 55°C for 30 s, and extension at 72°C for 30 s. Relative expression of the target gene was normalized to the expression of 18S. The standard graph of concentration versus Ct value for each gene of interest was plotted using a serially diluted cDNA. The starting quantity in the samples was determined using this standard graph. The starting quantity of each gene was divided by the starting quantity of 18S rRNA gene for normalization. The primer sequences used can be seen in Table II.

Statistical analyses

Statistical analysis of the averages of optical densities at 405 nm for the Alizarin Red staining assay and the relative gene expression from real-time PCR was performed using the independent sample student *t*-test. Statistical significance level was set at $p < 0.05$. For the Alizarin Red staining assay, each combination of medium and growth factor was run in hexaplicates and the experiments were repeated twice. The values shown in the figure 3 are averages of six replicates. The RNA was isolated from at least three different wells for each group to prepare cDNA and each sample of cDNA was run twice in real-time PCRs. The values shown in the graphs (Figures 4 and 5) are averages of triplicate experiments. The raw values (the OM value was not subtracted from other values) from Alizarin Red staining assay and real-time PCR were compared to assess the differences among the treatment groups. When the value of a gene/18S ratio in the combination group exceeded the sum of the two values of gene/18S ratios from VEGF group and BMP-6 group, it is defined as synergistic enhancement of expression of that gene.

Results

The characteristics of hADSCs

hADSCs were long, slender with a well-defined nucleus at the center of the cytoplasm (Figure 1A–D) and they could differentiate along adipogenic as well as osteogenic lineage (Figure 1E–H). All of the hADSCs expressed CD105, CD90, and CD73; none of them expressed CD45 and CD34; 23% of hADSCs

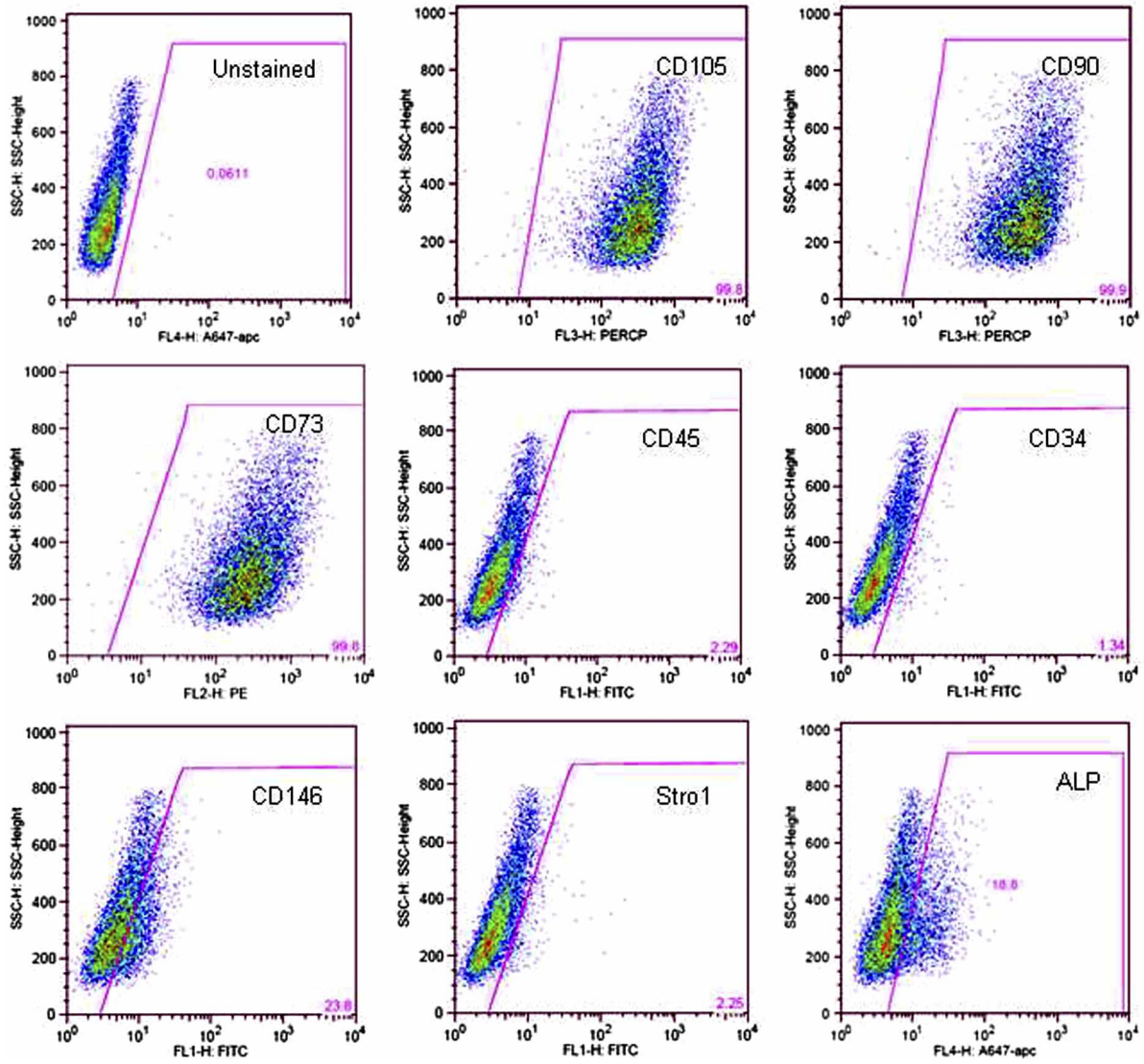

Figure 2. The hADSCs express MSC-specific markers. Using labeled monoclonal antibodies expression of MSC-specific markers was determined by flow cytometry.

expressed CD146 and 18% of the total population expressed alkaline phosphatase enzyme (Figure 2). We did not observe any hADSCs expressing Stro-1 receptor. hADSCs expressed VEGF receptors, TGF receptors, and BMP receptors (Figure 1I).

The combination of VEGF and BMP-6 enhances mineralization and ALP gene expression

VEGF and BMP-6 independently enhanced mineralization at day 14 (Figure 3) but VEGF was more effective in enhancing mineralization. Very low concentrations of VEGF (0.1 ng/ml) significantly ($p = 0.005$, ~ twofold in comparison with OM) enhanced mineralization. At day 14, the combination of 1 ng/ml VEGF plus 1 ng/ml BMP-6 increased mineralization significantly as compared to that observed in OM, 1 ng/ml VEGF, and 1 ng/ml BMP-6 groups ($p = 0.0005$, 0.048, and 0.0006). A corresponding increase in *ALP* gene expression was observed in the combined 1 ng/ml VEGF plus 1 ng/ml BMP-6 group (~ fivefold, $p = 0.0005$ in comparison with OM; Figure 4). Although mineralization increased in all the groups substantially at days 21 and 28 as compared to day 14, there were no statistically significant differences between OM and other groups containing VEGF or BMP-6 or both (Figure 3). However, *ALP* gene expression in the following groups was significantly higher than in the OM group at day 21: 1 ng/ml BMP-6, 1 ng/ml VEGF plus 1 ng/ml BMP-6, and 1 ng/ml VEGF plus 10 ng/ml BMP-6 ($p = 0.02$, 0.007, and 0.004, respectively; Figure 4). Overall, a combination of 1 ng/ml VEGF plus 1 ng/ml BMP-6 was the best at enhancing mineralization and *ALP* gene expression.

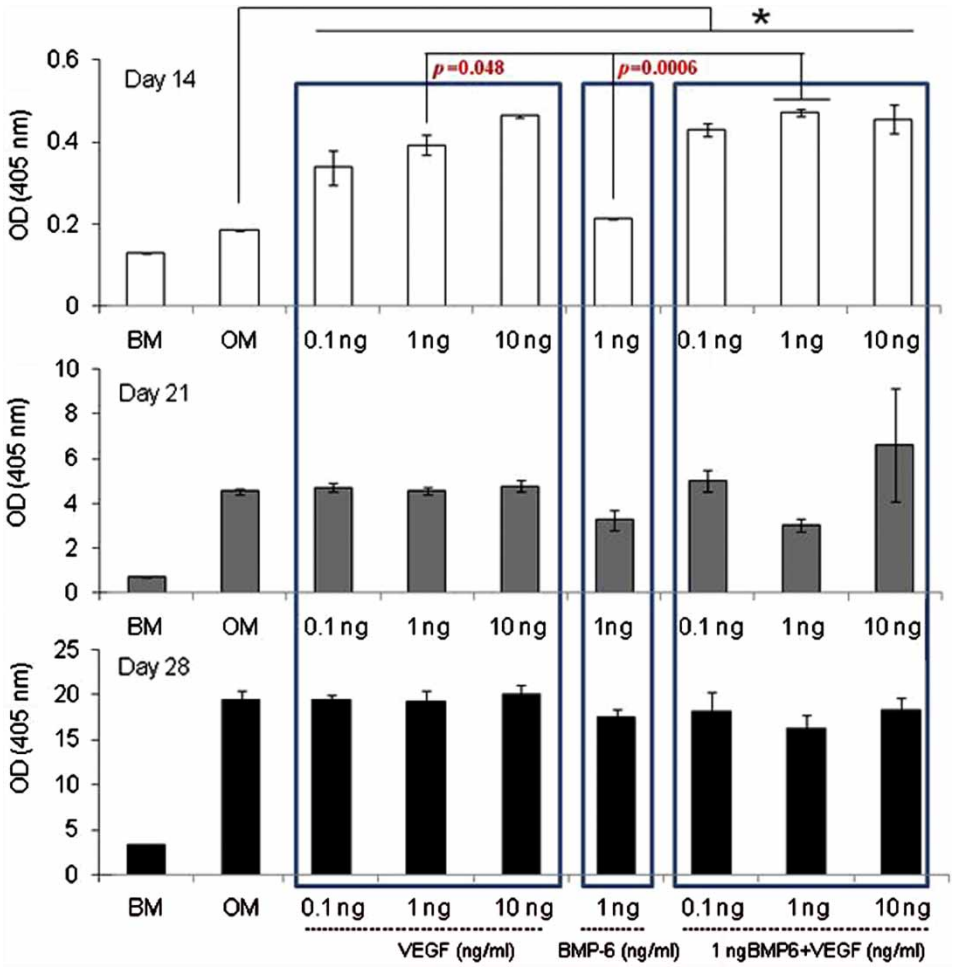

Figure 3. Combination of VEGF and BMP-6 enhances mineralization. hADSCs were grown in BM or OM or OM supplemented with the recombinant proteins. The mineralization was quantified after days 14, 21, and 28 by Alizarin Red staining and subsequent spectrophotometry at 405 nm. * denotes $p < 0.05$ in comparison with OM group.

The combination of VEGF and BMP-6 synergistically enhanced expression of COL1A1 but not osteocalcin

COL1A1 expression was comparable between day 14 (~ twofold in comparison with OM) and day 21 (~2.3-fold in comparison with OM) except in the VEGF plus BMP-6 groups (day 14: ~ twofold in comparison with OM; day 21, 0.1 ng VEGF plus 1 ng BMP-6: twofold, 1 ng VEGF plus 1 ng BMP-6: 3.3-fold, and 10 ng VEGF plus 1 ng BMP-6: 5.5-fold in comparison with OM). In the combination groups, *COL1A1* expression increased at day 21 (0.1 ng VEGF plus 1 ng BMP-6: no difference, 1 ng VEGF plus 1 ng BMP-6: 1.8-fold, and 10 ng VEGF plus 1 ng BMP-6: 2.7-fold) in comparison with that at day 14. Unlike VEGF alone or BMP-6 alone, the combination of VEGF and BMP-6 ($p = 0.002$ in comparison with OM) enhanced *COL1A1* gene expression by 5.5-fold in a dose-dependent manner at day 21 (Figure 4). The fold increase in *COL1A1* expression in 10 ng/ml VEGF plus 1 ng/ml BMP-6 group was more than the sum of fold increases in 10 ng/ml VEGF group (2.3-fold, $p = 0.031$ in comparison with OM) and 1 ng/ml BMP-6 group (2.6-fold, $p = 0.006$ in comparison with OM) revealing a synergistic enhancement in *COL1A1* expression in the combination group. A VEGF dose-dependent increase in *COL1A1* expression was observed in the combination groups and a maximum increase in *COL1A1* expression was observed at the ratio of VEGF:BMP-6 as 10:1 (~ twofold in comparison with OM; Figure 4). Interestingly, the use of similar VEGF:BMP-6 ratios failed to increase osteocalcin gene expression.

The synergistic increase in COL1A1 gene expression by the combination of VEGF and BMP-6 correlates with up-regulation of Runx2 and osterix genes

At day 21, the combination of VEGF:BMP-6 at a 10:1 ratio synergistically enhanced *COL1A1* gene expression and also synergistically enhanced transcription of osterix (~8.5-fold, $p = 0.015$ in comparison with OM; Figure 5). VEGF 10 ng/ml alone (~3.6-fold, $p = 0.18$ in comparison with OM) or BMP-6 1 ng/ml alone (~4.3-fold, $p = 0.06$ in comparison with OM) did not enhance osterix

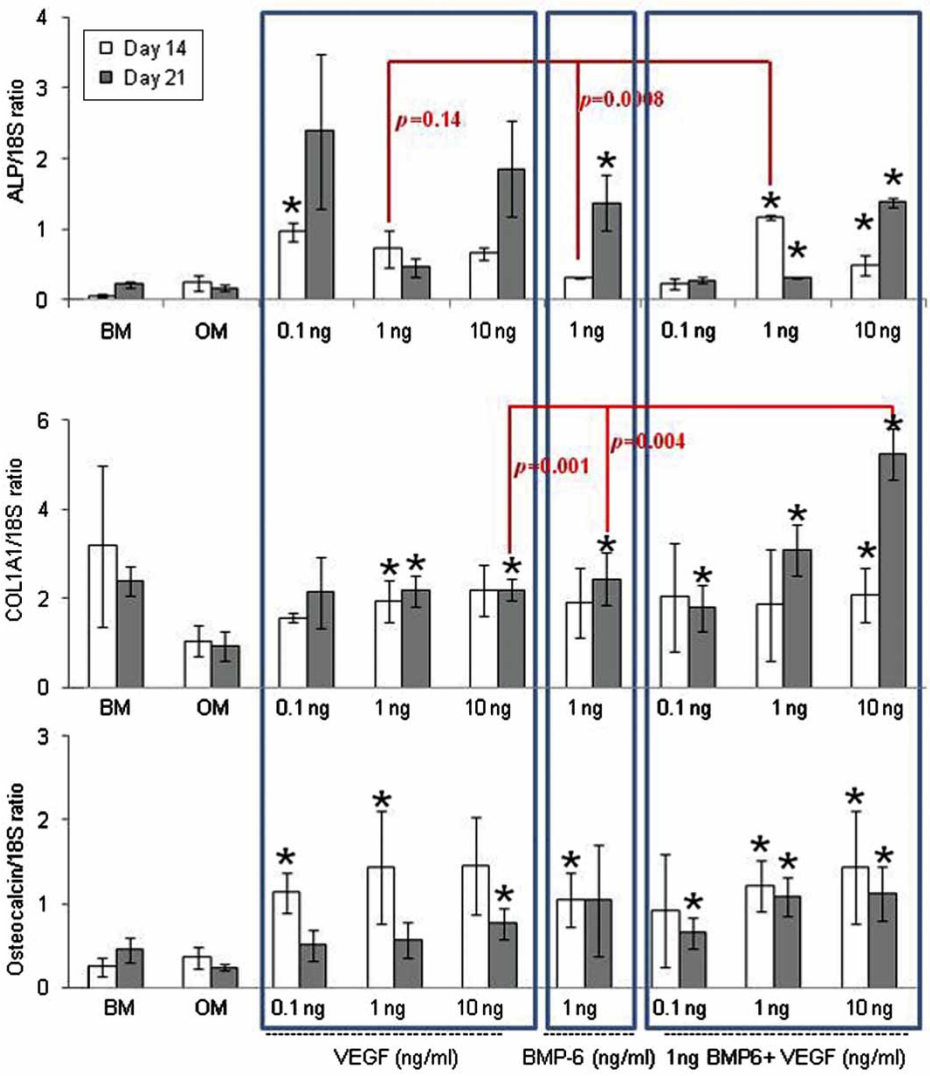

Figure 4. Cross-talk between VEGF and BMP-6 signaling pathways enhances expression of *ALP* and *COL1A1* genes but not osteocalcin gene. hADSCs were grown in BM or OM or OM supplemented with VEGF or BMP-6 or both. mRNA expression of *ALP*, *COL1A1*, and osteocalcin was quantitatively determined using real-time PCR. * denotes $p < 0.05$ in comparison with OM group at respective time point.

expression. We observed a similar trend (~ sevenfold, $p = 0.013$ in comparison with OM) in *Runx2* expression, but the difference between the combination group and VEGF group or BMP-6 group was not statistically significant. There was an upward trend in *Msx2* and *Dlx5* gene expression (Figure 5), plus there was a synergistic enhancement of *Msx2* (~ 12.8-fold, $p = 0.003$ in comparison with OM) at day 14 in this group. The synergistic enhancement in *Msx2* expression in the combination group was VEGF dose-dependent and maximum up-regulation was observed at the ratio of VEGF:BMP-6 as 10:1.

Up-regulation of Dlx5 gene requires simultaneous activation of VEGF and BMP-6 signaling pathways in hADSCs

At day 21, we observed ~ fivefold increase in *Dlx5* gene expression ($p = 0.0049$) in the 1 ng/ml VEGF plus 1 ng/ml BMP-6 group in comparison with the OM group. Importantly, addition of neither 1 ng VEGF alone nor 1 ng BMP-6 alone caused any significant increase in *Dlx5* expression (Figure 5). A 10:1 ratio of VEGF:BMP-6 also caused similar enhancement of osterix (Figure 5) gene. The data indicate that VEGF and BMP-6 signaling pathways cross-talk with each other in hADSCs.

Discussion

In recent years, *in vitro* studies have been conducted with hADSCs to help characterize their tissue regeneration potential as well as to determine which growth factors are best suited for cell-based therapies. BMP-6 has already been shown to induce chondrogenesis in hADSCs and may aid in cartilage regeneration for articular cartilage repair and reconstruction (Estes et al. 2006). Another

group conducting *in vitro* studies utilized an adenovirus vector to deliver Runx2, a transcription factor at the end of the BMP signaling pathway, to adipose tissue-derived stem cells (ADSCs; Zhang et al. 2006). They found a significant increase in alkaline phosphatase and mineral deposition as well as decreases in adipose tissue markers LPL (Lipoprotein lipase) and PPARgamma (Peroxisome proliferator-activated receptor gamma) further confirming the differentiation of ADSCs toward an osteogenic phenotype. Recent advancements in tissue engineering have taken these 2D *in vitro* cell cultures to a new dimension.

The creation of 3D tissue scaffolds has combined the efforts of bioengineers and molecular biologists in an attempt to better re-create the cell–cell interactions *in vivo* in an *ex vivo* model. One group compared 2D versus 3D cultures using hADSCs in the presence of osteogenic media and found that the 3D group had a 2.3-fold greater expression of alkaline phosphatase and a 2.9-fold greater expression of collagen I (Gabbay et al. 2006). Initial studies using tissue scaffolds, specifically the gelatin/B-tricalcium phosphate scaffold, have compared the osteogenic potential of hADSCs to human bone marrow-derived stem cells (hBMSCs) under the influence of BMP-2 and found similar results. Both groups demonstrated radiological densities similar to native bone suggesting that hADSCs may be a good alternative to hBMSCs for bone regeneration using these newer third-generation scaffolds (Weinand et al. 2011).

The purpose of this study was to investigate whether the combination of VEGF and BMP-6 enhanced osteoblastic differentiation of hADSCs *in vitro*. Our data revealed an increase in early mineralization (Figure 3) and expression of *ALP* and *COL1A1* (Figure 4) for the combination group, which proves that osteogenesis is enhanced by adding VEGF and BMP-6 to this MSC population *in vitro*.

Increases in mineralization and *ALP* expression, however, did not correlate with increases in expression of any particular transcription factor (Figure 5). Previous studies report that BMPs failed to enhance mineralization in hADSCs (Zuk et al. 2011), hBMSCs (Diefenderfer et al. 2003a,b; Osyczka et al. 2004; Mizuno et al. 2010), mouse BMSCs (Puleo 1997), or rat BMSCs (Hanada et al. 1997; Osyczka et al. 2004). We did not observe any significant increase in mineralization when VEGF or BMP-6 was added to the medium at day 21 or 28 (Figure 3). It is not known whether the MSCs used in these studies (Hanada et al. 1997; Puleo 1997; Diefenderfer et al. 2003a,b; Osyczka et al. 2004; Li et al. 2009; Zuk et al. 2011) were true MSCs and whether or not they expressed all necessary BMP receptors. We used hADSCs that satisfied the definition of true MSCs (Figure 2) and expressed all the necessary BMP

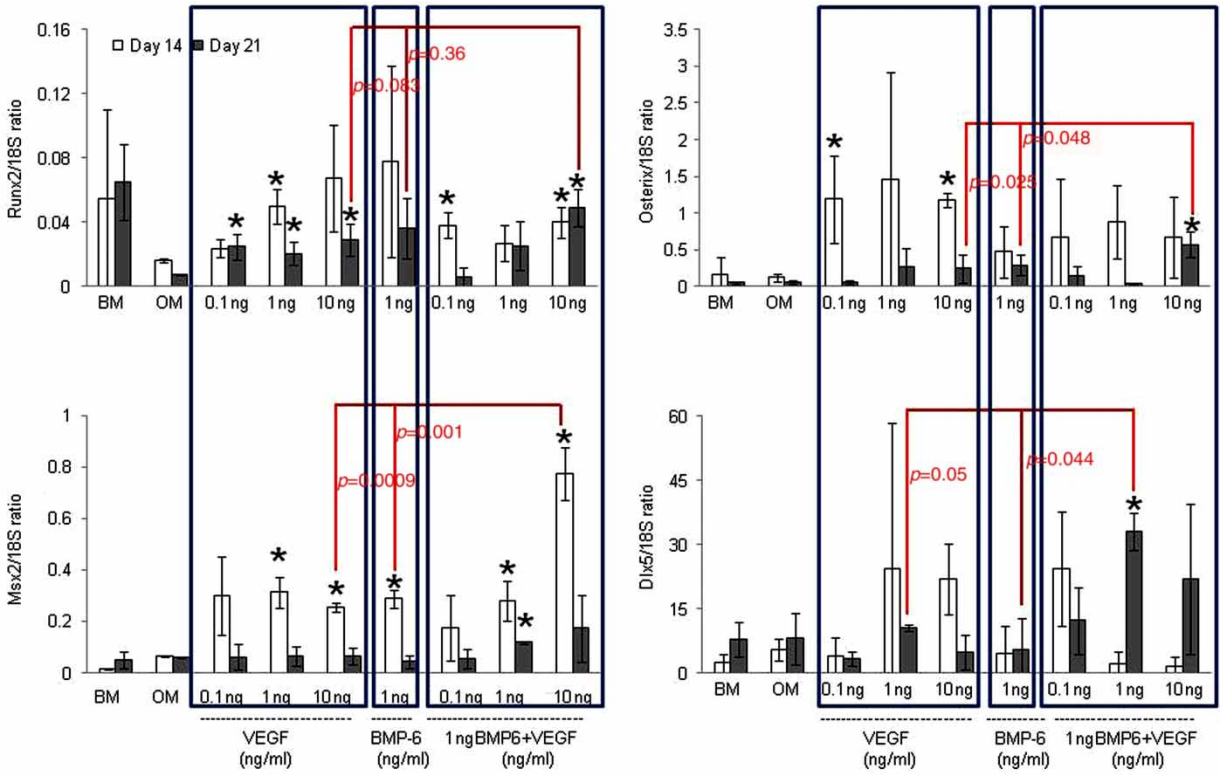

Figure 5. Enhancement of mRNA expression of osteogenic transcription factors through cross-talk between VEGF and BMP-6 signaling pathways. hADSCs were grown in BM or OM or OM supplemented with VEGF or BMP-6 or both. mRNA expression of Runx2, osterix, Msx2, and Dlx5 was quantitatively determined using real-time PCR. * denotes $p < 0.05$ in comparison with OM group at respective time point.

receptors (Figure 1). One study revealed that co-expression of *VEGF* and *BMP-4* genes in MSCs inhibited BMP-4-induced mineralization *in vitro*; plus MSC-induced osteogenesis *in vivo*; and the extent of VEGF inhibition was cell-type specific (Li et al. 2009). Differences in these studies indicate that the success of combined VEGF plus BMP therapy for MSC-mediated fracture repair may be dependent on the type of MSCs. Importantly, failure to significantly enhance mineralization should not imply that there is not a role for BMPs and MSCs in fracture healing.

The second phase of bone healing, soft callus formation, requires adequate amounts of collagen production. Bone is a complex material made up of a collagen matrix intermingled with rigid mineral crystals. The collagen provides toughness to the bone making it less brittle so that it better resists fracture and the mineral gives bone its stiffness (Turner 2006). The collagen cross-link formation can modulate the mineralization process of bone (Saito and Marumo 2010). To our surprise, many of the reports suggesting that MSCs do not respond to BMPs (Hanada et al. 1997; Puleo 1997; Diefenderfer et al. 2003a,b; Osyczka et al. 2004; Mizuno et al. 2010; Zuk et al. 2011) did not quantify *COL1A1* expression. The synergistic increase in *COL1A1* gene expression by the VEGF plus BMP-6 group (Figure 4) correlated with significant increases in *Runx2* and osterix mRNA levels plus an upward trend in *Msx2* and *Dlx5* expression at day 21 (Figure 5). *COL1A1* gene expression is modulated by several factors including Sp1 and Sp3 family transcription factors and *Runx2* (Chen et al. 1998; Kern et al. 2001; Verrecchia et al. 2001). Osterix is a recently identified Sp1 transcription factor family member required for the differentiation of progenitor cells into osteoblasts (Nakashima et al. 2002). Based on the findings of the current study and reports by other investigators (Lee et al. 2003; Matsubara et al. 2008), it is suggested that interaction between VEGF and BMP-6 signaling pathways increased mRNA levels of *Runx2* and the increased levels of *Runx2* led to enhanced osterix gene expression via up-regulation of *Msx2* and *Dlx5* (Figure 5) (Lee et al. 2003; Matsubara et al. 2008). Another important protein, OCN, is considered a marker of osteogenesis because it is produced only by osteoblasts. However, OCN protein is a known inhibitor of osteogenesis (Garcia et al. 2012). The combination group of VEGF plus BMP-6 did not increase mRNA levels of OCN which prevents inhibition of osteogenesis and allows maturation of hADSCs into an osteoblastic phenotype. This indicates that the *OCN* gene expression is not controlled by *Runx2*, osterix, *Msx2*, or *Dlx5* in hADSCs.

It is not clear at this moment how VEGF and BMP-6 signaling pathways interact with each other in a concerted effort to up-regulate transcription of osterix in hADSCs. Although these studies clearly suggest benefits of having both VEGF and BMPs for fracture repair, it is generally believed that enhanced angiogenesis is the primary mechanism for enhanced fracture repair. However, enhanced angiogenesis does not always correlate with enhanced osteogenesis (Matsumoto et al. 2009; Chen et al. 2011) and a recent report (Garcia et al. 2012) showed that there is no difference in levels of angiogenesis between fracture nonunions and unions. These findings argue that enhanced angiogenesis may not be the only mechanism by which combined VEGF plus BMP therapy promotes MSC-mediated fracture repair. Our data strongly suggest that interaction between VEGF and BMP-signaling pathways in MSCs enhances osteoblastic differentiation of hADSCs. As previously mentioned, hADSCs in combination with BMP incorporated onto 3D scaffolds may be the answer for difficult orthopedic cases involving large bone defects and nonunion.

With an aging population, future cell-based therapies will likely benefit from the fact that proliferation and osteogenic differentiation of hADSCs are less affected by age and multiple passages than BMSCs (Chen et al. 2011). Future *in vitro* studies to investigate cross-talk between VEGF and BMP-6 signaling pathways in hADSCs and *in vivo* studies using VEGF, BMP-6, and hADSCs for fracture repair will be necessary to determine the full potential of this approach.

Conclusion

To the best of our knowledge, this is the first study to investigate cross-talk between VEGF and BMP-6 signaling pathways in hADSCs. Our data indicate that simultaneous activation of VEGF and BMP-6 signaling pathways in hADSCs enhances expression of *COL1A1*, *osterix*, and *Dlx5* gene expression at specific VEGF:BMP-6 ratios. A thorough knowledge of signaling cross-talk between VEGF and BMP signaling pathways in MSCs may yield novel strategies for fracture repair.

Declaration of interest: The study was funded by research grants from the Orthopaedic Research and Education Foundation (OREF), USA and the Musculoskeletal Transplant Foundation (MTF), USA to QC. The authors report no conflicts of interest. The authors alone are responsible for the content and writing of the paper.

References

Boden SD, Liu Y, Hair GA, Helms JA, Hu D, Racine M, Nanes MS, Titus L. 1998. LMP-1, a LIM-domain protein, mediates BMP-6 effects on bone formation. Endocrinology 139(12):5125–5134.

Chen SJ, Artlett CM, Jimenez SA, Varga J. 1998. Modulation of human alpha1(I) procollagen gene activity by interaction with Sp1 and Sp3 transcription factors *in vitro*. Gene 215:101–110.

Chen HT, Lee MJ, Chen CH, Chuang SC, Chang LF, Ho ML, Hung SH, Fu YC, Wang YH, Wang HI, Wang GJ, Kang L, Chang JK. 2011. Proliferation and differentiation potential of human adipose-derived mesenchymal stem cells isolated from elderly patients with osteoporotic fractures. J Cell Mol Med 16(3):582–593.

Cui F, Wang X, Liu X, Dighe AS, Balian G, Cui Q. 2010. VEGF and BMP-6 enhance bone formation mediated by cloned mouse osteoprogenitor cells. Growth Factors 28(5):306–317.

Diefenderfer DL, Osyczka AM, Garino JP, Leboy PS. 2003a. Regulation of BMP-induced transcription in cultured human bone marrow stromal cells. J Bone Joint Surg Am 85:19–28.

Diefenderfer DL, Osyczka AM, Reilly GC, Leboy PS. 2003b. BMP responsiveness in human mesenchymal stem cells. Connect Tissue Res 44:305–311.

Dominici M, Le Blanc K, Mueller I, Slaper-Cortenbach I, Marini F, Krause D, Deans R, Keating A, Prockop DJ, Horwitz E. 2006. Minimal criteria for defining multipotent mesenchymal stromal cells. The International Society for Cellular Therapy position statement. Cytotherapy 8:315–317.

Estes BT, Wu AW, Guilak F. 2006. Potent induction of chondrocytic differentiation of human adipose-derived adult stem cells by bone morphogenetic protein 6. Arthritis Rheum 54(4): 1222–1232.

Gabbay JS, Heller JB, Mitchell SA, Zuk PA, Spoon DB, Wasson KL, Jarrahy R, Benhaim P, Bradley JP. 2006. Osteogenic potentiation of human adipose-derived stem cells in a 3-dimensional matrix. Ann Plast Surg 57(1):89–93.

Garcia P, Pieruschka A, Klein M, Tami A, Histing T, Holstein JH, Scheuer C, Pohlemann T, Menger MD. 2012. Temporal and spatial vascularization patterns of unions and nonunions: Role of vascular endothelial growth factor and bone morphogenetic proteins. J Bone Joint Surg Am 94:49–58.

Geiger F, Bertram H, Berger I, Lorenz H, Wall O, Eckhardt C, Simank HG, Richter W. 2005. Vascular endothelial growth factor gene-activated matrix (VEGF165-GAM) enhances osteogenesis and angiogenesis in large segmental bone defects. J Bone Miner Res 20(11):2028–2035, Epub 2005 Jul 5.

Gregory CA, Gunn WG, Peister A, Prockop DJ. 2004. An Alizarin red-based assay of mineralization by adherent cells in culture: Comparison with cetylpyridinium chloride extraction. Anal Biochem 329(1):77–84.

Hanada K, Dennis JE, Caplan AI. 1997. Stimulatory effects of basic fibroblast growth factor and bone morphogenetic protein-2 on osteogenic differentiation of rat bone marrow-derived mesenchymal stem cells. J Bone Miner Res 12:1606–1614.

Hanada K, Solchaga LA, Caplan AI, Hering TM, Goldberg VM, Yoo JU, Johnstone B. 2001. BMP-2 induction and TGF-beta 1 modulation of rat periosteal cell chondrogenesis. J Cell Biochem 81(2):284–294.

Hou H, Zhang X, Tang T, Dai K, Ge R. 2009. Enhancement of bone formation by genetically-engineered bone marrow stromal cells expressing BMP-2, VEGF and angiopoietin-1. Biotechnol Lett 31(8):1183–1189, Epub 2009 Apr 24.

Huang YC, Kaigler D, Rice KG, Krebsbach PH, Mooney DJ. 2005. Combined angiogenic and osteogenic factor delivery enhances bone marrow stromal cell-driven bone regeneration. J Bone Miner Res 20(5):848–857, Epub 2004 Dec 20.

Kang Q, Sun MH, Cheng H, Peng Y, Montag AG, Deyrup AT, Jiang W, Luu HH, Luo J, Luo J, Szatkowski JP, Vanichakarn P, Park JY, Li Y, Haydon RC, He TC. 2004. Characterization of the distinct orthotopic bone-forming activity of 14 BMPs using recombinant adenovirus-mediated gene delivery. Gene Ther 11: 1312–1320.

Kempen DH, Lu L, Heijink A, Hefferan TE, Creemers LB, Maran A, Yaszemski MJ, Dhert WJ. 2009. Effect of local sequential VEGF and BMP-2 delivery on ectopic and orthotopic bone regeneration. Biomaterials 30(14):2816–2825, Epub 2009 Feb 20.

Kern B, Shen J, Starbuck M, Karsenty G. 2001. Cbfa1 contributes to the osteoblast-specific expression of type I collagen genes. J Biol Chem 276:7101–7107.

Krause U, Seckinger A, Gregory CA. 2011. Assays of osteogenic differentiation by cultured human mesenchymal stem cells. Methods Mol Biol 698:215–230.

Kubo S, Cooper GM, Matsumoto T, Phillippi JA, Corsi KA, Usas A, Li G, Fu FH, Huard J. 2009. Blocking vascular endothelial growth factor with soluble Flt-1 improves the chondrogenic potential of mouse skeletal muscle-derived stem cells. Arthritis Rheum 60(1):155–165.

Lee MH, Kwon TG, Park HS, Wozney JM, Ryoo HM. 2003. BMP-2-induced Osterix expression is mediated by Dlx5 but is independent of Runx2. Biochem Biophys Res Commun 309: 689–694.

Li X, Cui Q, Kao C, Wang GJ, Balian G, 2003a. Lovastatin inhibits adipogenic and stimulates osteogenic differentiation by suppressing PPARgamma2 and increasing Cbfa1/Runx2 expression in bone marrow mesenchymal cell cultures. Bone 33:652–659.

Li JZ, Li H, Sasaki T, Holman D, Beres B, Dumont RJ, Pittman DD, Hankins GR, Helm GA. 2003b. Osteogenic potential of five different recombinant human bone morphogenetic protein adenoviral vectors in the rat. Gene Ther 10:1735–1743.

Li G, Corsi-Payne K, Zheng B, Usas A, Peng H, Huard J. 2009. The dose of growth factors influences the synergistic effect of vascular endothelial growth factor on bone morphogenetic protein 4-induced ectopic bone formation. Tissue Eng Part A 15(8): 2123–2133.

Matsubara T, Kida K, Yamaguchi A, Hata K, Ichida F, Meguro H, Aburatani H, Nishimura R, Yoneda T. 2008. BMP2 regulates Osterix through Msx2 and Runx2 during osteoblast differentiation. J Biol Chem 283:29119–29125.

Matsumoto T, Cooper GM, Gharaibeh B, Meszaros LB, Li G, Usas A, Fu FH, Huard J. 2009. Cartilage repair in a rat model of osteoarthritis through intraarticular transplantation of muscle-derived stem cells expressing bone morphogenetic protein 4 and soluble Flt-1. Arthritis Rheum 60(5):1390–1405.

Mizuno D, Agata H, Furue H, Kimura A, Narita Y, Watanabe N, Ishii Y, Ueda M, Tojo A, Kagami H. 2010. Limited but heterogeneous osteogenic response of human bone marrow mesenchymal stem cells to bone morphogenetic protein-2 and serum. Growth Factors 28:34–43.

Nakashima K, Zhou X, Kunkel G, Zhang Z, Deng JM, Behringer RR, de Crombrugghe B. 2002. The novel zinc finger-containing transcription factor osterix is required for osteoblast differentiation and bone formation. Cell 108:17–29.

Osyczka AM, Diefenderfer DL, Bhargave G, Leboy PS. 2004. Different effects of BMP-2 on marrow stromal cells from human and rat bone. Cells Tissues Organs 176:109–119.

Patel ZS, Young S, Tabata Y, Jansen JA, Wong ME, Mikos AG. 2008. Dual delivery of an angiogenic and an osteogenic growth factor for bone regeneration in a critical size defect model. Bone 43(5):931–940, Epub 2008 Jul 14.

Peng H, Wright V, Usas A, Gearhart B, Shen HC, Cummins J, Huard J. 2002. Synergistic enhancement of bone formation and healing by stem cell-expressed VEGF and bone morphogenetic protein-4. J Clin Invest 110(6):751–759.

Peng H, Usas A, Olshanski A, Ho AM, Gearhart B, Cooper GM, Huard J. 2005. VEGF improves, whereas sFlt1 inhibits, BMP2-induced bone formation and bone healing through modulation of angiogenesis. J Bone Miner Res 20(11):2017–2027, Epub 2005 Jul 18.

Puleo DA. 1997. Dependence of mesenchymal cell responses on duration of exposure to bone morphogenetic protein-2 *in vitro*. J Cell Physiol 173:93–101.

Sacchetti B, Funari A, Michienzi S, Di Cesare S, Piersanti S, Saggio I, Tagliafico E, Ferrari S, Robey PG, Riminucci M, Bianco P. 2007. Self-renewing osteoprogenitors in bone marrow sinusoids

can organize a hematopoietic microenvironment. Cell 131: 324–336.

Saito M, Marumo K. 2010. Collagen cross-links as a determinant of bone quality: A possible explanation for bone fragility in aging, osteoporosis, and diabetes mellitus. Osteoporos Int 21: 195–214.

Samee M, Kasugai S, Kondo H, Ohya K, Shimokawa H, Kuroda S. 2008. Bone morphogenetic protein-2 (BMP-2) and vascular endothelial growth factor (VEGF) transfection to human periosteal cells enhances osteoblast differentiation and bone formation. J Pharmacol Sci 108(1):18–31, Epub 2008 Sep 6.

Scharpfenecker M, van Dinther M, Liu Z, van Bezooijen RL, Zhao Q, Pukac L, Löwik CW, ten Dijke P. 2007. BMP-9 signals via ALK1 and inhibits bFGF-induced endothelial cell proliferation and VEGF-stimulated angiogenesis. J Cell Sci 120(Pt 6): 964–972, Epub 2007 Feb 20.

Tallone T, Realini C, Böhmler A, Kornfeld C, Vassalli G, Moccetti T, Bardelli S, Soldati G. 2011. Adult human adipose tissue contains several types of multipotent cells. J Cardiovasc Transl Res 4:200–210.

Turner CH. 2006. Bone strength: Current concepts. Ann NY Acad Sci 1068:429–446.

Verrecchia F, Rossert J, Mauviel A. 2001. Blocking Sp1 transcription factor broadly inhibits extracellular matrix gene expression *in vitro* and *in vivo*: Implications for the treatment of tissue fibrosis. J Invest Dermatol 116:755–763.

Wang X, Cui F, Madhu V, Dighe AS, Balian G, Cui Q. 2011. Combined VEGF and LMP-1 delivery enhances osteoprogenitor cell differentiation and ectopic bone formation. Growth Factors 29(1):36–48.

Weinand C, Nabili A, Khumar M, Dunn JR, Ramella-Roman J, Jeng JC, Jordan MH, Tabata Y. 2011. Factors of osteogenesis influencing various human stem cells on third-generation gelatin/B-tricalcium phosphate scaffold material. Rejuvenation Res 14(2):185–194, Epub 2011 Jan 16.

Young S, Patel ZS, Kretlow JD, Murphy MB, Mountziaris PM, Baggett LS, Ueda H, Tabata Y, Jansen JA, Wong M, Mikos AG. 2009. Dose effect of dual delivery of vascular endothelial growth factor and bone morphogenetic protein-2 on bone regeneration in a rat critical-size defect model. Tissue Eng Part A 15(9): 2347–2362.

Zhang X, Yang M, Lin L, Chen P, Ma KT, Zhou CY, Ao YF. 2006. Epub 2006 Sep 11 Runx2 overexpression enhances osteoblastic differentiation and mineralization in adipose-derived stem cells *in vitro* and *in vivo*. Calcif Tissue Int 79(3):169–178.

Zuk P, Chou YF, Mussano F, Benhaim P, Wu BM. 2011. Adipose-derived stem cells and BMP2: Part 2.BMP2 may not influence the osteogenic fate of human adipose-derived stem cells. Connect Tissue Res 52:119–132.